Saturation of color forces and nuclear binding

Hiroshi Matsuoka and Dennis Sivers
High Energy Physics Division, Argonne National Laboratory, Argonne, Illinois 60439
(Received 3 September 1985)

We discuss an approach to understanding the saturation of forces in chromodynamics. Our formulation is suggested by the observation that many lattice-gauge-theory calculations give results well approximated by considering the dynamics of stringlike flux tubes. By looking at multiquark Green's functions in the strong-coupling, quenched, approximations of lattice chromodynamics we find examples of configuration mixing which can allow the binding of color-singlet hadrons into larger composite systems. We surmise that this configuration mixing is crucial to the understanding of nuclear binding. As a simple example we discuss the binding of two mesons composed of heavy, static, quarks into a deuteronlike object. Our results suggest that the magnitude of nuclear binding can be deduced by measuring a finite number of Wilson-loop configurations in lattice QCD.

I. INTRODUCTION

The assembly of protons and neutrons into larger composite objects plays such a crucial role in nature that it is important to understand the nuclear binding force from first principles. There now exist strong indications that quantum chromodynamics (QCD) provides the underlying theoretical basis for the strong interactions[1] and, hence, it is compelling to look for an explanation of nuclear binding in QCD. The task will not necessarily be straightforward. QCD is a gauge theory which describes the interactions of fundamental quarks and gluons. The binding of quarks and gluons into color-singlet hadrons is already known to be a topic which cannot be treated in perturbation theory.[2] Therefore, the idea that one can calculate the properties of nuclei in terms of the short-distance interactions of quarks and gluons seems quite remote.

There is, however, a viable alternative to perturbation theory for some observables in QCD. The lattice approximation of a gauge-field theory involves the replacement of the space-time continuum by a discrete number of points. The formulation of the theory on these points can be done in a way which explicitly preserves gauge invariance and allows a continuation between the strong-coupling regime and the weak-coupling regime.[3] In lattice calculations, many observables can be reliably estimated by sampling a finite number of gauge-field configurations. The formulation therefore yields quantitative, systematically improvable predictions.

A simpler question then arises. Can one construct observables in lattice QCD which can be used to understand the existence of nuclear binding? From the point of view of QCD, the problem of nuclear binding can be seen as merely one aspect of the general problem of the long-distance saturation of the chromodynamic force. Other aspects of this subject include the properties of "exotic" hadrons, the possible existence of hybrid meson-glueball states, and the study of other types of nonminimal color-singlet states.[4] The dramatic suggestion that stable strange matter could account for the dark mass of the Universe or special cosmic-ray events[5] shows how the subject of color-force saturation can lead to new areas of speculation. Understanding the saturation of forces in QCD involves looking at general multiquark states, examining how quarks cluster into color-singlet hadrons, and deducing the residual interactions between the color singlets. This basic problem was first addressed in nonrelativistic potential models. However, several authors have pointed out the difficulty that two-body quark potentials lead to a long-range van der Waals force between two color-singlet hadrons which is in violent disagreement with experiment.[6] Subsequently, multiquark systems have been examined in the MIT bag model[7] and in simple string models.[8] These models explicitly postulate dynamical mechanisms which naturally isolate color singlets and, hence, remove the problem of long-range van der Waals forces. However, they do not solve the problem in a manner which can be seen to be a natural consequence of the underlying QCD dynamics.

Suppose we want to study color-force saturation in nonperturbative QCD. We can, in principle, look at general multiquark Green's functions in the lattice approximation to QCD. We recall that for a heavy static $Q\bar{Q}$ pair one can deduce the effective interquark potential in the quenched approximation (ignoring the effects of light quarks) by measuring Wilson loops[9] of different sizes. We find that the study of multiquark systems can be done in a similar manner by looking at more complicated Wilson surfaces. We will illustrate this by looking at the surfaces which give the "potential" for a $Q\bar{Q}Q\bar{Q}$ system. The $Q\bar{Q}Q\bar{Q}$ system is chosen for study since it is the simplest multiquark system which gives nontrivial results concerning color saturation. In addition, it has been argued that this system can serve as a prototype for simple nuclei[10] and it is therefore interesting to look at its behavior in lattice QCD as a guide to what we might encounter in more complicated systems.

In this paper we look at the Euclidean Green's function for a $Q\bar{Q}Q\bar{Q}$ system in the strong-coupling, quenched approximation to lattice QCD. The Euclidean-space Green's function consists of a 2×2 matrix in color space with entries which can be calculated by tiling the ap-

propriate Wilson surfaces. Since the strong-coupling limit of the theory is known to give a string picture, where color flux between sources is confined to stringlike flux tubes, it is not surprising that we can reproduce the general clustering properties of string models. However, there exists another important element in the complete calculation since the strong-coupling expansion gives a calculable overlap between different color-space configurations. We interpret this as configuration mixing familiar from simple multichannel quantum mechanics. It is easy to convince oneself that configuration mixing allows for the formation of a composite "nucleus" with lower overall energy than two individual hadrons.

Our sample calculation is done in the quenched approximation where all light quarks are suppressed so it is not convenient to describe the resultant hadron-hadron binding in terms of meson exchange as is customarily done in nuclear-physics models. To understand physical hadronic systems, we must obviously also include meson-exchange effects. On the lattice, it turns out that one can calculate configuration mixing without reference to the strong-coupling expansion by measuring different types of Wilson surfaces in Monte Carlo simulations. In fact, if these measurements can be done in sufficient generality, taking into account dynamic quark degrees of freedom through the fermion determinant, it should be possible to include meson exchange and mixing effects on a comparable footing. We believe that this will be necessary in order to achieve a "first-principles" understanding of nuclear binding from QCD.

The remainder of this paper is organized as follows. In Sec. II we set up the $Q\bar{Q}Q\bar{Q}$ Green's function in the strong-coupling limit of Euclidean lattice QCD. Section III gives the results obtained by diagonalizing the color-space operator. Section IV discusses the extension of the approach beyond the limits of the strong-coupling approximation and some aspects of the extension to other multiquark systems. Section V attempts to make contact with standard nuclear-physics techniques and formulates some tentative conclusions.

II. THE STRONG-COUPLING EXPANSION AND A SIMPLE EXAMPLE OF COLOR-FORCE SATURATION

The strong-coupling approximation is a useful beginner's tool for the understanding of lattice-gauge-theory results.[3] For non-Abelian gauge theories, the strong-coupling approximation forces color flux to be confined to stringlike flux tubes. Unlike weak coupling or "ordinary" perturbation theory, the expansion in $(1/g^2)$ for strong coupling has a finite radius of convergence for many types of observables. High-order calculations in $(1/g^2)$ can be continued using several approximation schemes such as Padé approximates[11] to extend the region of applicability still further. As g^2 gets smaller for any given theory, one encounters, at some point, a roughening transition which for some observables invalidates continuation of the strong-coupling results. At very small values of g^2, lattice-based perturbation expansions are valid.[12] For the calculation of a given observable, one must consider the renormalization effects through the relation $g^2 \to g^2(a)$ where a denotes the underlying lattice spacing. To make contact with continuum physics, we must eventually consider the extrapolation $a \to 0$ and $g^2(a) \to 0$. However, this does not invalidate *all* considerations based on the dynamics of the strong-coupling limit. Monte Carlo simulations can be used to connect the strong-coupling and the weak-coupling regimes. Measurements of Wilson loops suggest strongly that the flux-tube picture of the strong-coupling approximation is valid[13] for large loops even though the strong-coupling string tension cannot be naively extrapolated to $g^2=0$. This indicates that strong coupling may provide a good starting point to examine the long-distance properties of more general multiquark systems.

We will define a lattice gauge theory for SU_3 with no dynamic quarks in terms of the Wilson action

$$S(U)=\frac{6}{g^2}\sum_i [1-\tfrac{1}{3}\mathrm{Re}\,\mathrm{Tr}(U_\square)] , \tag{2.1}$$

where $U_\square = U_{\hat{i}_1} U_{\hat{i}_2} U_{\hat{i}_3} U_{\hat{i}_4}$ and the path $\hat{i}_1 \cdots \hat{i}_4$ surrounds a fundamental plaquette. The generating functional is defined

$$Z=\int d[U]\exp[-S(U)] . \tag{2.2}$$

We can calculate the expectation value of local observables (observables which involve only a finite number of points and links) by

$$\langle O\rangle = Z^{-1}\int d[U]O(U)\exp[-S(U)] . \tag{2.3}$$

These expectation values involve the group-invariant Haar measure defined by

$$d[U]=d[U^{-1}]=d[UV] . \tag{2.4}$$

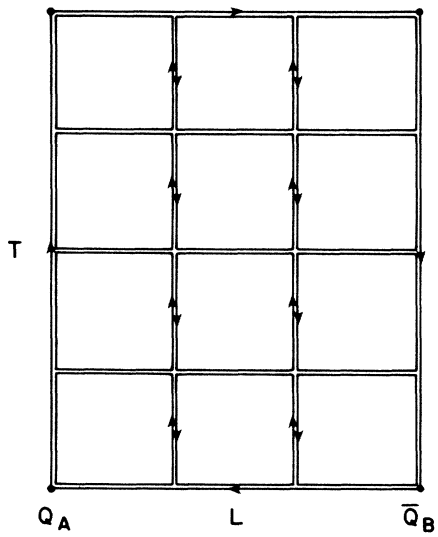

FIG. 1. Wilson loop $W(L,T;g^2)$ in the strong-coupling limit. It takes a minimum of $N=LT/a^2$ fundamental plaquettes to tile the area in such a way that the group integral does not vanish.

The group integrals for SU_3 can be evaluated using

$$\int d[U]=1\,,$$
$$\int d[U]U=\int d[U]U^{\dagger}=0\,, \tag{2.5}$$
$$\int d[U]U_{ij}U^{\dagger}_{kl}=\tfrac{1}{3}\delta_{il}\delta_{jk}\,.$$

The strong-coupling approximation consists of taking the expansion of the exponential

$$\exp[-S(U)]\cong 1-\frac{6}{g^2}[\Omega]+\cdots \tag{2.6}$$

with

$$\Omega=\sum_i[1-\tfrac{1}{3}\mathrm{Re\,Tr}(U_{\square})]\,, \tag{2.7}$$

and evaluating the integral (2.3) as a power series in $1/g^2$.

One of the simplest operators which can be calculated in the strong-coupling expansion is a Wilson loop $W(L,T;g^2)$. This operator can be considered to represent the creation of a massive, static $Q\bar{Q}$ pair separated by a distance L at time $t=0$, the propagation of this static pair through Euclidean time to $t=T$ and its subsequent annihilation. As pictured in Fig. 1, the lowest-order contribution to this operator in the strong-coupling approximation consists of tiling the minimal area enclosed by the loop, with $LT/a^2=N$ elementary plaquettes in order to get a nonvanishing group integral

$$\lim_{g^2\to\infty}\langle W(L,T,g^2)\rangle\sim\left[\frac{1}{3g^2}\right]^{LT/a^2}=\exp(-\sigma LT) \tag{2.8}$$

with

$$\sigma=\sigma(a,g^2)=\frac{1}{a^2}\ln(3g^2)\,. \tag{2.9}$$

The parameter σ with dimensions (length)$^{-2}$ can be interpreted as a string tension giving rise to a linear confining potential between widely separated color sources. When one considers the renormalization of the theory one must assume that physical quantities such as σ are independent of the underlying bare parameters in the calculation. This means a relationship between a and g^2 of the form

$$\lim_{g^2\to\infty}a(g^2)\sim[\ln(3g^2)/\sigma]^{1/2}\,. \tag{2.10}$$

Higher-order terms in the strong-coupling expansion lead to corrections to $\sigma(a,g^2)$ in (2.9) and, hence, higher-order corrections to $a(g^2)$.

For large T, one can interpret the coefficient in (2.8) as

$$\langle W(L,T;\sigma)\rangle=\exp[-V(L)T]\,, \tag{2.11}$$

where $V(L)$ is the potential between the static quarks. The strong-coupling result, therefore, leads to a linear potential

$$\lim_{L\to\infty}V_{Q\bar{Q}}(L)\sim\sigma L\,. \tag{2.12}$$

We have gone over this familiar result in order to introduce the nomenclature we will be using to discuss the

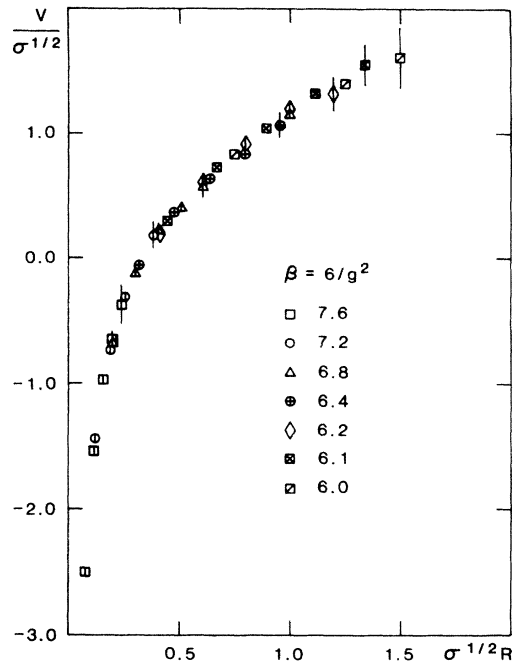

FIG. 2. Otto and Stack's potential from Monte Carlo data on a $12^3\times 16$ lattice. In Ref. 9 they have fit these data to the phenomenological potential given in Eq. (2.14) of the text.

$Q\bar{Q}Q\bar{Q}$ system. We want to emphasize, however, that the strong-coupling result (2.12) is approximately valid for the large-distance behavior of the $Q\bar{Q}$ potential. Figure 2 shows results from the Monte Carlo simulations of Otto and Stack[9] for the $Q\bar{Q}$ potential. These involve calculations done in the "scaling region" of $g^2\lesssim 1$ where the strong-coupling expansion is not valid. However, the large-distance behavior of the potential is still linear. If we are interested in the behavior of systems with

$$L\gtrsim 5\,\mathrm{GeV}^{-1} \tag{2.13}$$

then a linear approximation is reasonably valid. Otto and Stack[9] give a fit to their Monte Carlo data of the form

$$V(L)=\frac{\alpha}{L}+\sigma L \tag{2.14}$$

with $\alpha=0.25\pm0.02$ and $\sigma^{1/2}=260\pm10$ MeV which gives a $Q\bar{Q}$ potential with a wider range of validity than (2.12). When we consider the large-distance limit of multiquark "potentials" in the remainder of this paper, however, we will assume that (2.12) is an adequate approximation for $V_{Q\bar{Q}}$.

A simple example of $Q\bar{Q}Q\bar{Q}$ dynamics

We can now turn to the $Q\bar{Q}Q\bar{Q}$ system. To simplify the geometry we will assume that the massive scalar static quarks are confined to the x-y plane and are located at the corners of a rectangle as shown in Fig. 3. The labels $ABCD$ denote distinct "flavors." In the strong-coupling limit there are two flux configurations which associate $Q\bar{Q}$ pairs into color-singlet "mesons." These are shown in Figs. 3(b) and 3(c). There are different ways to parametrize the color-space degrees of freedom for this

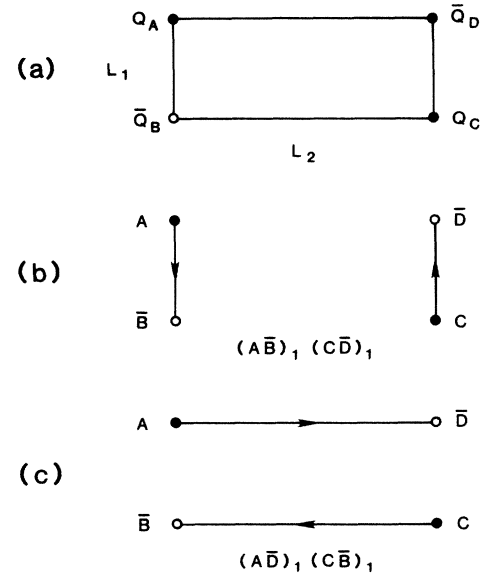

FIG. 3. The sketch in (a) shows the geometry of the $Q\bar{Q}Q\bar{Q}$ system discussed in the text. The two quarks and two antiquarks are held rigidly at the corners of a rectangle as shown. The two distinct ways of grouping the quarks into color-singlet mesons are shown in the sketches labeled (b) and (c) by drawing a flux line between the Q and $\bar{Q}$ which form a color singlet. The two configurations are labeled $(A\bar{B})_1(C\bar{D})_1$ and $(A\bar{D})_1(C\bar{B})_1$.

system. One basis, in color space, is given by

$$|(Q_A\bar{Q}_B)_1(Q_C\bar{Q}_D)_1\rangle_1 = |(A\bar{B})_1(C\bar{D})_1\rangle_1\ ,$$
$$|(Q_A\bar{Q}_B)_8(Q_C\bar{Q}_D)_8\rangle_1 = |(A\bar{B})_8(C\bar{D})_8\rangle_1\ , \tag{2.15}$$

and another basis

$$|1\rangle = |(Q_A\bar{Q}_B)_1(Q_C\bar{Q}_D)_1\rangle = |(A\bar{B})_1(C\bar{D})_1\rangle\ ,$$
$$|2\rangle = |(Q_A\bar{Q}_D)_1(Q_C\bar{Q}_B)_1\rangle = |(A\bar{D})_1(C\bar{B})_1\rangle\ . \tag{2.16}$$

It is easy to convince oneself that the states (2.16) are more convenient for the quantum mechanics of the strong-coupling limit where one has to take into account both the color carried by the quarks and the orientation of the color flux. At short distances, where one can ignore the extra complications associated with the flux the set (2.15) may be more convenient. For quarks at a single point, there are algebraic relations between the color components of (2.15) and (2.16). For the remainder of this paper we will be using the basis vectors (2.16) for describing this system. In any dynamical approximation consistent with confinement, we can see that these are adiabatic states for the Hamiltonian at large distances.

We can easily see that the Euclidean-space Green's function which corresponds to the creation of the $Q\bar{Q}Q\bar{Q}$ system at $t=0$ and its annihilation at $t=T$ is then a 2×2 matrix in color space. The generalization of the Wilson loop for a single $Q\bar{Q}$ pair is the operator which is a 2×2 matrix

$$W_{IJ}(L_1,L_2,T,\sigma)$$

with $I,J=1,2$ and the color states defined in (2.16). The components of this operator are indicated in Fig. 4. The diagonal components correspond to the product of two Wilson loops. The off-diagonal components correspond to the connected surfaces shown in Figs. 4(b) and 4(c).

In the strong-coupling limit, we can compute the con-

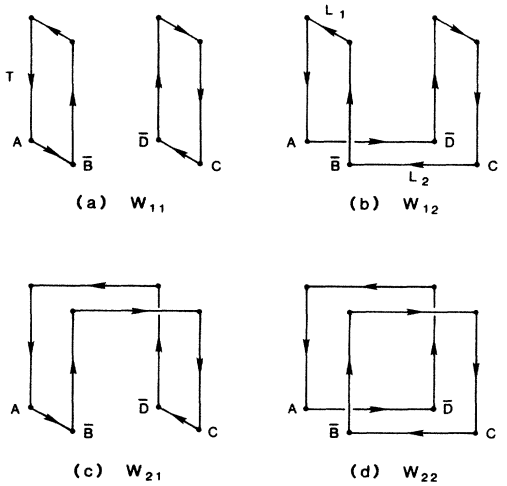

FIG. 4. These sketches show the Wilson surfaces whose values correspond to the elements in the Euclidean Green's function for the $Q\bar{Q}Q\bar{Q}$ system.

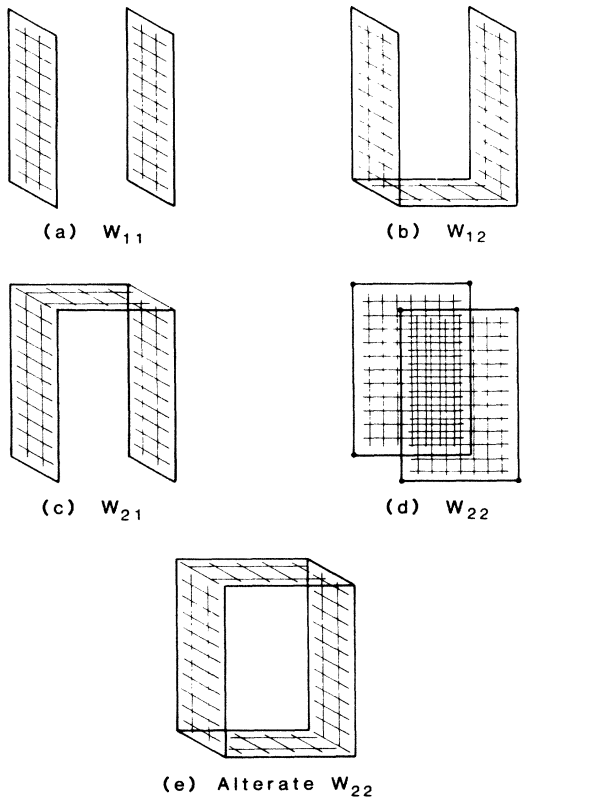

FIG. 5. Shading or crosshatching in sketches indicate minimal tilings in strong coupling which lead to (2.17). In the limit $(L_2-L_1)T > L_1L_2$ the minimal tiling for W_{22} switches to that shown in (e). This indicates that in this limit the configuration (2) is unstable against decay into state 1. The propagator for $2\to2$ consists of jumping to state 1, propagating for time T and then jumping back to state 2. For the discussion in the text, it is more instructive to consider the tiling in (d).

tribution of each of these Wilson surfaces, by tiling the minimal area enclosed by the loops with fundamental plaquettes. In order to show some definite results, we will assume $L_1 < L_2$ and $(L_2 - L_1)T < L_1 L_2$. Following the same arguments which led to (2.8), we then have

$$W_{IJ} \cong e^{-2\sigma L_1 T} \begin{vmatrix} 1 & e^{-\sigma L_1 L_2} \\ e^{-\sigma L_1 L_2} & e^{-2\sigma(L_2 - L_1)T} \end{vmatrix} . \tag{2.17}$$

The tilings which give this minimal area are shown in Fig. 5. Note that if we look at $(L_2 - L_1)T > L_1 L_2$ then the minimal tiling of the surface which corresponds to W_{22} changes to that shown in Fig. 5(e). We want to make some simple observations about (2.17). In the configuration discussed above, it is clear the off-diagonal elements are small compared to the diagonal ones. This confirms the general picture that the color-singlet mesons interact only weakly. However, we cannot completely ignore the configuration mixing represented by the off-diagonal elements. They tell us that the physical states do not consist of independent mesons but that there exists a linear combination of the states $|(A\bar{B})_1(C\bar{D})_1\rangle$ and $|(A\bar{D})_1(C\bar{B})_1\rangle$ which has a lower energy than the two mesons. Clearly, if we are interested in the binding of color-singlet hadrons, we must consider these mixing effects.

III. CONFIGURATION MIXING AS A CONTRIBUTION TO BINDING

In Sec. II we showed how the Euclidean-space Green's function for a $Q\bar{Q}Q\bar{Q}$ system can be thought of as a 2×2 matrix operator in color space. In the strong-coupling limit with two meson states as an appropriate basis, we can see how the tiling of Wilson surfaces of different topologies gives the entries in this matrix. In the $Q\bar{Q}Q\bar{Q}$ system, we are therefore confronted with the classic example of a two-channel problem in quantum mechanics where the appropriate physical states can be deduced by diagonalizing this operator. Our simple model indicates that the mixing will, in general, be small and the main dynamical feature of the system is the confinement of the $Q\bar{Q}$ pairs into hadrons. However, the fact that mixing can occur allows the formation of a larger bound state involving all four sources.

Since we are treating Q's and $\bar{Q}$'s as simple static color sources, we must examine W_{IJ} for a range of L_1 and L_2 in order to understand the dynamics of the system. In particular, we need to be able to deal smoothly with the case $(L_2 - L_1) \to 0$ in order to describe all allowed configurations. It turns out that the tilings of the Wilson surfaces leading to (2.17) do not adequately deal with the degeneracy of allowed configurations. For the off-diagonal elements of W_{IJ}, we must also consider tilings of the Wilson surface such as that drawn in Fig. 6. In these tilings, the spacelike surface with area $L_1 L_2$ occurs not only at $t = 0$ or $t = T$ but at any t_a subject to $0 \le t_a \le T$. In the strong-coupling limit, the contribution of each such tiling is

$$\delta(L_1, L_2, t_a, T) = e^{-\sigma L_1 L_2} e^{-2\sigma L_2 (T - t_a)} e^{-2\sigma L_1 t_a} . \tag{3.1}$$

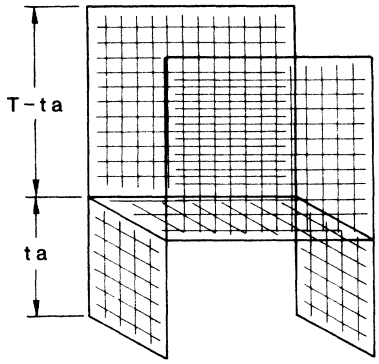

FIG. 6. The T dependence of the operator is not properly described by the tilings in Fig. 5 which ignore the degeneracy associated with the fact that the spacelike surface of area $L_1 L_2$ can occur at any time $0 \le t_a \le T$. Summing over configurations leads to (3.2) and the matrix operator (3.3).

Summing over these configurations gives

$$\epsilon(L_1, L_2 T) = e^{-\sigma L_1 L_2} \left[\frac{e^{-2\sigma L_1 T} - e^{-2\sigma L_2 T}}{2\sigma(L_2 - L_1)a} \right] , \tag{3.2}$$

where $a = a(g^2, \sigma)$ denotes the fundamental lattice spacing and is assumed to be small compared to the size of the figure. Notice that this form is smoothly behaved in the limit $L_2 - L_1 \to 0$,

$$\epsilon(L, L, T) = e^{-\sigma L^2}(T/a) e^{-2\sigma L T} . \tag{3.3}$$

After realizing that (2.17) is not strictly correct, we can improve our calculation of the matrix to

$$W = \begin{bmatrix} e^{-2\sigma L_1 T} & \epsilon \\ \epsilon & e^{-2\sigma L_2 T} \end{bmatrix} \tag{3.4}$$

with ϵ given by (3.2). We now proceed to diagonalize (3.4) and write $D = RWR^{-1}$ where R is a 2×2 rotation matrix and

$$\begin{aligned} \tan 2\theta &= \frac{2\epsilon}{e^{-2\sigma L_1 T} - e^{-2\sigma L_2 T}} \\ &= \frac{2e^{-\sigma L_1 L_2}}{2\sigma(L_2 - L_1)a} . \end{aligned} \tag{3.5}$$

The diagonal elements are then

$$\begin{aligned} D_{11} &= \frac{e^{-2\sigma L_1 T} + e^{-2\sigma L_2 T}}{2} \\ &\quad + \frac{e^{-2\sigma L_1 T} - e^{-2\sigma L_2 T}}{2} \cos 2\theta + \epsilon \sin 2\theta , \\ D_{22} &= \frac{e^{-2\sigma L_1 T} + e^{-2\sigma L_2 T}}{2} \\ &\quad - \frac{e^{-2\sigma L_1 T} - e^{-2\sigma L_2 T}}{2} \cos 2\theta - \epsilon \sin 2\theta . \end{aligned} \tag{3.6}$$

From (3.2) we see that ϵ is small. For the case of small mixing $(L_1 \neq L_2)$, we can write

$$D_{11} \cong W_{11} + \frac{\epsilon^2}{W_{11} - W_{22}} = W_{11}[1 + \chi_-(T)] ,$$
$$D_{22} \cong W_{22} - \frac{\epsilon^2}{W_{11} - W_{22}} = W_{22}[1 + \chi_+(T)] . \tag{3.7}$$

From (3.2)

$$\chi_\pm(T) = \frac{e^{-2\sigma L_1 L_2}}{4\sigma^2 a^2} \frac{1 - e^{\mp 2\sigma(L_2 - L_1)T}}{(L_2 - L_1)^2} . \tag{3.8}$$

In the case of small mixing we can therefore deduce the energy shift attributed to mixing to be approximately

$$-\frac{1}{T}(\ln D_{11} - \ln W_{11}) \cong \mp \frac{e^{-2\sigma L_1 L_2}}{2\sigma a^2} \frac{1}{(L_2 - L_1)} . \tag{3.9}$$

In the limit of $L_2 = L_1 = L$, we have $\sin 2\theta = 1$ and ϵ given by (3.3). This gives

$$D_{11} = e^{-2\sigma LT} + \epsilon = e^{-2\sigma LT}(1 + e^{-\sigma L^2 T/a}) ,$$
$$D_{22} = e^{-2\sigma LT} - \epsilon = e^{-2\sigma LT}(1 - e^{-\sigma L^2 T/a}) . \tag{3.10}$$

From this we can deduce the energy shift

$$-\frac{1}{T}(\ln D_{11} - W_{11}) \cong \mp e^{-\sigma L^2} \frac{1}{a} . \tag{3.11}$$

The mixing is maximized for $L_2 = L_1 = L$. For both (3.9) and (3.10) we see that the amount of the energy shift depends sensitively on the interquark spacing because of the factor $\exp(-\sigma L_1 L_2)$. For fixed L_1, the "binding" potential falls off exponentially with L_2. This rapid falloff guarantees that at asymptotic separations, the correct physical states consist of bound mesons with no residual forces.

Putting in some numbers, we find that this type of configuration mixing has the ability to quantitatively account for a significant amount of nuclear binding. For $L_1 = L_2 = L$ we show the order of magnitude of

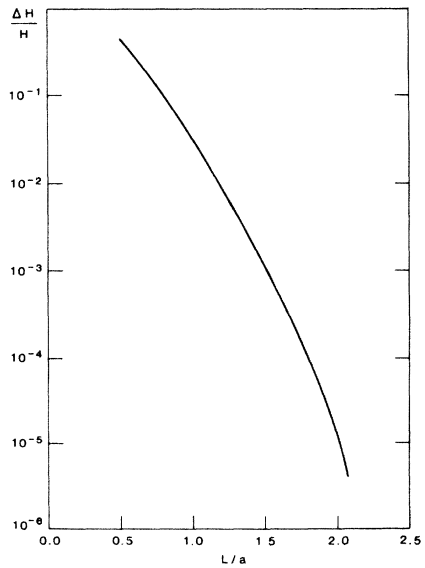

FIG. 7. $\Delta H/H$ vs L/a from (3.12). For physical values of separations we get energy shifts of 10^{-3}.

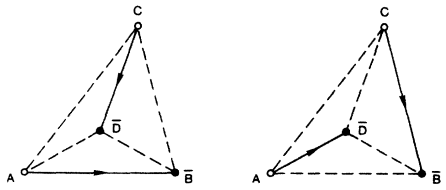

FIG. 8. The four sources $A, \bar{B}, C, \bar{D}$ determine the vertices of an irregular tetrahedron in three-space. The six edges of the tetrahedron have lengths $L_{A\bar{B}}$, L_{AC}, $L_{A\bar{D}}$, $L_{C\bar{B}}$, $L_{C\bar{D}}$, and $L_{\bar{B}\bar{D}}$. The T=const slices of Wilson surfaces involve the $L_{A\bar{B}}$ and $L_{C\bar{D}}$ or the $L_{A\bar{D}}$ and $L_{C\bar{B}}$ edges as shown.

$$\frac{\Delta H}{H} \cong \frac{\exp(-\sigma L^2)}{2\sigma L a} \tag{3.12}$$

for various values of (L/a) in Fig. 7. For "physical" values of interquark separation we achieve binding energies in the MeV range. Surprisingly, the overall picture of color force saturation which emerges from the strong-coupling limit of lattice QCD seems to have several nice features which naturally account for physical phenomena.

It is obvious that there is a long way to go from the study of our simple example of static spinless color sources before we can deal with physical states of nuclear matter. For example, one aspect of the $Q\bar{Q}Q\bar{Q}$ problem which needs to be treated more completely before drawing firm conclusions involves the geometry of the system. We have, for simplicity, been treating the color sources as occupying the corners of a rectangle. As sketched in Fig. 8, we should in general consider the Q's and $\bar{Q}$'s to be located at the corners of an irregular tetrahedron in three-space.

The more complicated geometrical setup can still be understood using the basic ideas discussed above but there are some features which require extra care. The diagonal elements of the Euclidean-space Green's function still involve two disjoint Wilson loops. However, the loops may intertwine. To see how this can happen we can consider the configuration shown in Fig. 9 where, again, the four color sources are confined to a plane. In this configura-

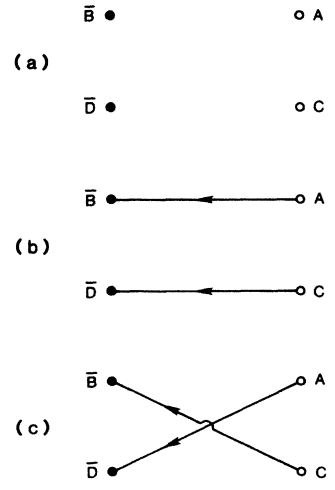

FIG. 9. Another orientation of sources confined to a plane. One of the flux configurations which separates the system into mesons involves flux crossing as shown.

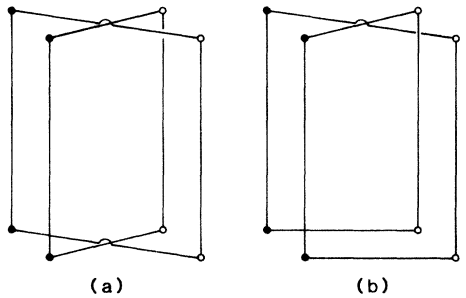

FIG. 10. Wilson surfaces for diagonal (a) and off-diagonal (b) propagators involving crossed flux orientations.

tion, however, the two quarks and the two antiquarks occupy adjacent corners of a rectangle. Flux lines connecting quarks and antiquarks are drawn and, it is obvious that, in one of the possible configurations, the lines overlap. The types of Wilson surfaces which must be calculated for this geometry are shown in Fig. 10.

Obviously, to attempt to calculate the contribution of these diagrams in strong-coupling lattice approximation, we must take into account the non-Abelian nature of color flux. For general configurations of Q's and $\bar{Q}$'s, tilings of the surfaces with junctions as shown in Fig. 11 must be considered.

We want to point out that it is possible to do a more systematic and thorough treatment of the $Q\bar{Q}Q\bar{Q}$ system which takes into account the full complexity of the geometry of the static sources. The basic conclusion which emerges from our simple numerical example above—that configuration mixing in the two-channel meson-meson basis leads to the possibility of binding these mesons into a larger object—remains valid. We will not deal in detail with all these geometries at this time since we are not yet trying to construct a realistic model for the $Q\bar{Q}Q\bar{Q}$ potential but only to introduce the basic concepts and calculating tools. Note that we also have to consider the sensitivity of our calculation to the approximations of the strong-coupling expansion. We will address some aspects of the problems of extrapolating away from strong coupling in the next section.

IV. MIXING AND THE STRONG-COUPLING APPROXIMATION

There are several facets of our calculation of Sec. III which depend on the strong-coupling expansion. Since the details of continuum physics should not depend on

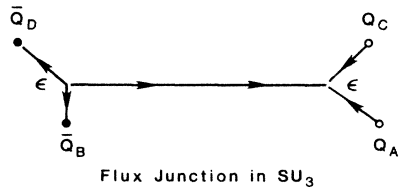

FIG. 11. Tiling of Wilson surfaces in many configurations involve the non-Abelian nature of the charges and the fact that $\epsilon^{ijk}q_jq_k$ transforms like an antiquark. For the special geometry in our simple problem, these flux configurations are not important.

any artificial lattice approximation scheme, we have to consider the extrapolation away from this limit to see whether our results remain valid. Fortunately, it will not ultimately be necessary to rely on specific arguments concerning the extrapolation away from strong coupling since it is possible to do Monte Carlo explicit simulations which can statistically measure the appropriate Wilson surfaces.

Some aspects of this continuation can be dealt with in a fairly straightforward manner. We would like to discuss these in order to show some of the things which need to be done. The first aspect is the normalization of the meson wave functions, the second involves the correlation between Wilson loops. Finally, we would like to look at a simple argument which suggests that the strong-coupling approximation underestimates mixing.

The meson wave functions

In the strong-coupling limit, we can consider a "meson" to be a $Q\bar{Q}$ pair joined by a string non-Abelian flux tube. As we go away from the strong-coupling limit while keeping the color sources fixed, the color flux is no longer confined to a narrow tube. We can define the state

$$\Psi(Q\bar{Q},L)=\sum_i c_i \mid Q(0),\text{flux } i,\bar{Q}(L)\rangle \ , \tag{4.1}$$

where the label i refers to all the allowed flux configurations connecting the Q and $\bar{Q}$. When we calculate the Wilson surfaces drawn in Fig. 4, the spacelike lines at $t=0$ and $t=T$ represent projections of the meson state onto the straight-line flux state. As we go away from the strong-coupling limit, this projection becomes smaller and the ratio between the Wilson operator and the meson propagator diminishes. A little thought shows that the important result of configuration mixing found in Sec. III depends on the ratio of the off-diagonal elements to the diagonal elements in W_{IJ} as given in (3.4). We can still calculate these elements using the Wilson surfaces as shown in Fig. 5. The ratio of the Wilson surfaces to the elements of the exact Euclidean-space Green's function denoted by G_{IJ} is given in the form

$$\frac{G_{12}}{G_{11}}=\frac{W_{12}}{W_{11}}\left[\frac{\Psi(Q\bar{Q},L_1)\Psi(Q\bar{Q},L_2)}{\Psi_0(Q\bar{Q},L_1)\Psi_0(Q\bar{Q},L_2)}\right] \times\left[\frac{\Psi_0(Q\bar{Q},L_1)\Psi_0(Q\bar{Q},L_1)}{\Psi(Q\bar{Q},L_1)\Psi(Q\bar{Q},L_1)}\right], \tag{4.2}$$

where Ψ_0 represents the "straight-line" flux state where all coefficients in (4.1) except c_0 are set to zero. As long as the ratio of these normalization factors depends only weakly on L_1 and L_2 then the ratio of the Wilson surfaces can be used to calculate the mixing in the Green's function as in Sec. III. We do not have to depend on the strong-coupling expansion to calculate these operators. We can investigate the ratios in (4.2) by changing the edges of loops with different topologies in Monte Carlo simulations.

Other interactions

In our example above, the diagonal elements of the $Q\bar{Q}Q\bar{Q}$ Green's function correspond to the independent

propagation of noninteracting mesons. In the limit of strong coupling, there is no correlation between the two disjoint Wilson loops of Fig. 5. However, as we extrapolate away from the strong-coupling limit, this no longer remains true.

We can study the correlation function between disjoint Wilson loops numerically. In principle, this is similar to studies involving the propagators of "glueball" states. The correlation length should be dominated by the mass of the lowest glueball state. Estimates of this mass

$$m^G_{0^{++}} \simeq 0.66 \pm 0.03 \text{ GeV} \tag{4.3}$$

have been made using Monte Carlo data.[14] Its value remains more uncertain than is indicated in (4.3) because the scaling (behavior with coupling) of the data on the glueball mass and the scaling of the data on the string tension are not consistent. Without a single β function which can describe both kinds of data, it is premature to say that an overall scale is set which allows the mass of the lowest glueball to be related to the string tension. However, the mass scale (4.3) indicates that there will be a force with range (σ) even in the one-channel approximation.

In the language of potentials, glueball exchange generates a force between mesons just like the standard one-meson-exchange potential used to describe the NN force. In the quenched approximation or the absence of dynamical quarks this is the only type of exchange allowed between heavy mesons. The configuration mixing calculated in Sec. III does not correspond to the exchange of a heavy $Q\bar{Q}$ pair since this would be suppressed by an extra Yukawa factor

$$Y = \exp(-2m_Q L) . \tag{4.4}$$

Configuration mixing leads to a component of the binding force more akin to covalent bonding in atomic physics than to the exchange potentials used in nuclear models.

Enhanced mixing at low g^2

We have discussed some of these effects briefly to indicate that there is some reason to believe the overall result. There is one dynamical effect which we do think will prove to be important and which leads us to believe that our quantitative estimates of configuration mixing may be too low. In the strong-coupling limit, the tiling of the spacelike surface which allowed the mixing necessarily introduced a factor

$$\chi(L_1, L_2) = \exp(-\sigma L_1 L_2) . \tag{4.5}$$

This can be understood in a simple flux model as shown in Fig. 12. As we go toward smaller couplings there exist correlated configurations for which the factor

$$\chi(L_1, L_2) = \exp(-\sigma A') \tag{4.6}$$

with $A' \ll L_1 L_2$. Our main expectation concerning the results of the continuation away from strong coupling is that configuration mixing will increase as g^2 becomes smaller. A simple parametrization of this general effect would be to replace the value of σ which occurs in (3.11) or (3.12) as a measure of the energy shift by a value $\sigma' < \sigma$.

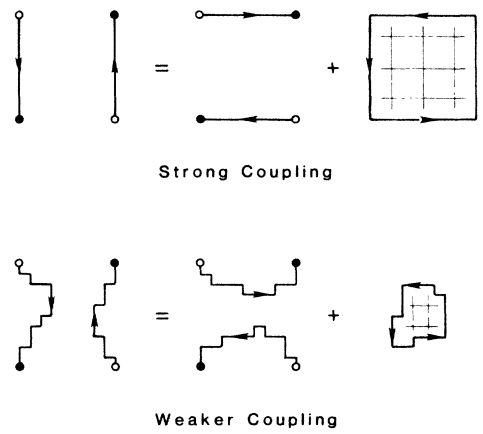

FIG. 12. As we go away from the strong-coupling limit so that flux lines are not restricted to their minimum length, there exist correlated flux configurations for which the area A' of a spacelike surface which needs to be tiled is less than $A = L_1 L_2$.

We would like to emphasize that it will not ultimately be necessary to rely on unsupported theoretical arguments. The Wilson surfaces involved in our calculation can be measured using lattice Monte Carlo techniques. If these measurements can be done with the same sort of accuracy that has been done for the meson spectrum[15] or for the $Q\bar{Q}$ potential,[9] then we will have a fundamental measurement of configuration mixing in chromodynamics. We are currently setting up these types of Monte Carlo studies and will report on them elsewhere.

To summarize our estimates concerning the extrapolation away from the strong-coupling limit we find that there are several effects which must be considered. It seems probable that the amount of configuration mixing will be larger than our simpler estimate.

V. QCD AND NUCLEAR STRUCTURE

The traditional approach to understanding the binding of color-singlet hadrons into nuclei starts with fundamental pointlike nucleons and a phenomenological potential.[16] The essential components of the potential include a long-range component associated with one-meson exchange and a short-range repulsive barrier.[17] The details of the potential can vary as more and more dynamical features are input.

We do not wish to examine this traditional approach in great detail. We simply do not believe that it constitutes a satisfactory starting point for the study of nuclei and that its overall validity must ultimately depend on the results of a thorough understanding of quantum chromodynamics. If available theoretical tools cannot succeed in describing the confinement of quarks and gluons into color-singlet hadrons and the binding of hadrons into extended nuclei in terms of the underlying dynamics we must remain skeptical of the basic theory of chromodynamics.

In our study of the $Q\bar{Q}Q\bar{Q}$ Green's function in lattice chromodynamics we have isolated a dynamical mechanism which cannot be easily described in terms of the ex-

change of mesons or glueballs. This means that there is at least one aspect of QCD that would necessarily remain hidden if one tried to construct an effective theory of nuclear binding involving only hadronic degrees of freedom. It is essential to our approach that mesons consist of $Q\bar{Q}$ pairs and that the fundamental force involves color. The details of our calculation, in particular the quantitative results which depend on the strong-coupling approximation, are less important than the fact that we can set up a program for calculating multiquark operators which can give quantitative information about nuclear binding.

The generalization of our approach to the $6Q$ system is reasonably straightforward once one considers the extra complexity associated with the additional constituents. With six static quarks, there are ten independent ways of forming two color-singlet baryons. The Green's function is then a 10×10 matrix in the basis of these two baryon states. The calculation of the elements in this operator in terms of the appropriate Wilson surfaces and the diagonalization of this 10×10 matrix follows along the methods outlined in Secs. II and IV. Of course, the types of different geometrical configurations which must be considered is larger than for $Q\bar{Q}Q\bar{Q}$. Not only the location of the quarks, but also the placement of the flux lines on the spacelike boundaries of the Wilson surfaces, must be varied. Existing calculations of the baryon spectrum in the quenched approximation to lattice QCD (Ref. 15) have not dealt with the baryonic wave function in great detail. This must be done at some level before one can address the question of configuration mixing.

We have tried to emphasize in this paper that the question of color-force saturation in non-Abelian field theories is a very important one which deserves to be addressed with a full range of theoretical techniques. A lattice calculation of multiquark Green's functions offers some new insight into the problem. The fact that a mechanism for the binding of hadrons appears in the strong-coupling limit and that this binding can be calculated in terms of the value of simple operators constitutes an important new result.

ACKNOWLEDGMENTS

We have benefited immensely from discussions with S. Gottlieb, L. Heller, and H. Lipkin. This work was supported by the U.S. Department of Energy, Division of High Energy Physics, under Contract No. W-31-109-ENG-38.

[1]The most succinct argument for QCD is the beautiful way an SU_3 theory of quarks and gluons combines with the $SU_2\times U_1$ electroweak theory. Of course, measurements of jet observables in $e^+e^-\rightarrow$hadrons and $\bar{p}p\rightarrow$hadrons probe the short-distance behavior of the strong interactions and support QCD. Reviews on the current status of QCD include F. Wilczek, Ann. Rev. Nucl. Part. Sci. **32**, 177 (1982); E. Eichten, I. Hinchliffe, K. Lane, and C. Quigg, Rev. Mod. Phys. **56**, 579 (1984).

[2]It can be shown that any calculation of hadronic masses for hadrons involving light quarks implies $m_H\propto\exp(-A/g^2+\cdots)$. See, for example, C. Callan, G. Dashen, and D. Gross, Phys. Rev. D **19**, 1826 (1979).

[3]Introductions to lattice gauge theories include J. Kogut, Rev. Mod. Phys. **55**, 775 (1983); J.-M. Drouffe and J.-B. Zuber, Phys. Rep. **102**, 1 (1983); M. Creutz, L. Jacobs, and C. Rebbi, *ibid.* **95**, 201 (1983).

[4]For a discussion of exotic hadrons in the quark model, see J. Weinstein and N. Isgur, Phys. Rev. Lett. **48**, 659 (1982); T. Barnes, F. E. Close, and G. Monaghan, Nucl. Phys. **B198**, 380 (1982).

[5]E. Witten, Phys. Rev. D **30**, 272 (1984).

[6]H. J. Lipkin, Phys. Lett. **45B**, 267 (1973); P. M. Fishbane and M. T. Grisaru, *ibid.* **74B**, 98 (1978); T. Appelquist and W. Fischler, *ibid.* **77B**, 405 (1978); R. S. Willey, Phys. Rev. D **18**, 270 (1978).

[7]C. DeTar, Phys. Rev. D **17**, 323 (1978).

[8]C. J. Horowitz, E. J. Moniz, and J. W. Negele, Phys. Rev. D **31**, 1689 (1985); N. Isgur and J. Paton, *ibid.* **31**, 2910 (1985).

[9]See, for example, S. Otto and J. Stack, Phys. Rev. Lett. **52**, 2328 (1984).

[10]L. Heller and J. A. Tjon, Phys. Rev. D **32**, 755 (1985); See also, L. Heller, in *Quarks and Nuclear Forces,* edited by D. C. Fires and B. Zeitnitz (Springer Tracts in Modern Physics, Vol. 100) (Springer, Berlin, 1982), p. 145.

[11]M. Falcioni *et al.*, Nucl. Phys. **B190**, 782 (1981); Phys. Lett. **102B**, 270 (1981); **108B**, 331 (1982).

[12]M. Creutz, Phys. Rev. D **23**, 1815 (1981).

[13]J. Ambjørn, P. Olesen, and C. Peterson, in *Gauge Theory on a Lattice,* proceedings of the Argonne National Laboratory Workshop, 1984, edited by C. Zachos, W. Celmaster, E. Kovacs, and D. Sivers (National Technical Information Service, Springfield, Virginia, 1984), p. 147.

[14]Ph. De Forcrand, G. Schierholz, H. Schneider, and M. Teper, Phys. Lett. **160B**, 137 (1985); G. Schierholz and M. Teper, *ibid.* **136B**, 64 (1984).

[15]D. Weingarten, Phys. Lett. **109B**, 57 (1982); Nucl. Phys. **B215**, 1 (1983); H. Hamber and G. Parisi, Phys. Rev. Lett. **47**, 1792 (1981); C. Bernard, T. Draper, and K. Olynyk, Phys. Rev. D **27**, 227 (1982); R. Gupta and A. Patel, Phys. Lett. **124B**, 94 (1983), Nucl. Phys. **B226**, 152 (1983); K. Bowler, G. Pawley, D. Wallace, E. Marinari, and F. Rapuano, *ibid.* **B220[FS8]**, 137 (1983); H. Lipps, G. Martinelli, R. Petronzio, and F. Rapuano, Phys. Lett. **126B**, 250 (1983); A. Hasenfratz, P. Hasenfratz, Z. Kunszt, and C. B. Lang, *ibid.* **110B**, 289 (1982); J. P. Gilchrist, H. Schneider, G. Shierholz, and M. Teper, *ibid.* **136B**, 87 (1984).

[16]For example, M. Lacombe *et al.*, Phys. Rev. C **21**, 861 (1980).

[17]A. D. Jackson, Ann. Rev. Nucl. Part. Sci. **33**, 105 (1983); B. Day, Rev. Mod. Phys. **50**, 495 (1978); S. O. Bäckman and G. E. Brown, Phys. Rep. **124**, 1 (1985).